Numerical Investigation of a Ferrofluid Boundary Layer on a Flat Plate

Arthur A. R. Campos
Rafael G. Gontijo
Francisco R. Cunha
University of Brasilia, Department of Mechanical Engineering,Fluid Mechanics of Complex Flows Lab - VORTEX,
72campos@gmail.com, rafaelgabler@gmail.com, frcunha2@gmail.com

Abstract. *This paper performs a numerical study of a magnetic fluid flow over a flat plate. The goal is to explore several new features of this boundary layer problem. The main difference from classical laminar boundary layers is that in the present work the flow interacts with controllable magnetic fields. This interaction opens the doors for several new possible applications, such as boundary layer control and fluid friction reduction. In order to perform this study we developed a non commercial research code based on the finite difference method using a vorticity-stream function formulation. The proposed formulation avoids the necessity of using a pressure-velocity coupling algorithm as long as we are dealing with a barotropic fluid flow. The numerical method is described in details and the results are compared with a rigorous scaling analysis performed by the authors. The code validation is done by comparing the non magnetic problem with the classical Blasius theoretical solution. The idea of this paper is to show that the interaction between the magnetic and velocity fields leads to a new and interesting flow with several possible patterns depending on the magnetic field boundary conditions. We also explore different constitutive equations for describing the magnetic stress using different generalizations of the Maxwell stress tensor. We intend through this work to study how different constitutive relations affect the main vector fields of the problem. A detailed study on the magnetization evolutive equation is also presented and discussed.*

Keywords: *Vorticity-Stream Function. magnetic fluid, magnetization model, Maxwell's stresses, constitutive equation.)*

1. INTRODUCTION

Boundary layer theory is the field of hydrodynamics that studies the flow of both liquids and gases past a solid body. In 1904 Prandtl(Acheson, 2009)(Schlichting, 2000), addressed this problem by arguing that the no-slip condition on the surface of a solid body would create a near wall thin layer where the velocity gradient would be so strong that the viscous effects in this region could not be neglected. Since then the study of flows with small viscosity has been divided into two different parts, one inside the boundary layer where viscosity plays a significant role in the flow, and one outside the boundary layer where viscous effects can be neglected without significant effects.

In terms of engineering, boundary layers are almost everywhere from air planes, wind turbines, sewers systems, auto mobiles and even our home computer depends on this flow mechanism. Controlling the boundary layer is of crucial importance for a working engineer. For example a well design air foil is one where it minimizes drag and increases lift without stalling or a good sewer system design is one where the pressure loss along the pipes are not so big that a new pump must be added and so on.(Granger, 1997)

Despite it's wide range of applications, boundary layers are not so easy to work with. Most of the time the intrinsic parameters that will influence on the effects of the boundary layer are not so easy to design and sometimes even impossible. The most important parameter that governs this phenomena is the ratio between the inertial forces with the viscous forces, also known as the Reynolds number in honor to Osborne Reynolds (Acheson, 2009)(Granger, 1997) who studied the effects of viscosity in great depth.

In 1963 NASA developed a new kind a fluid that could interact with a magnetic field so that they could be moved in micro-gravity environments. This new material has opened a whole new branch of hydrodynamics, now known as ferrohydrodynamics, as well as lots of new applications in science and engineering(Stephen, 1965). Despite the fact that the initial goals of FHD were focused on moving a fluid with controllable magnetic fields, nowadays we can find many other fields where FHD plays an important role.

Ferrofluids consists on nano magnetic particles, usually magnetite, maghemite or hematite, mixed with a liquid carrier forming a colloidal suspension (Rosenweig, 2014). This material can show instabilities if proper care is not taken, the diameter of each particle must be small enough so that the Brownian forces of the carrier liquid can overcome sedimentation. Also these particles must have a proper surfactant coating in order to avoid clustering and precipitation induced by particle agglomeration.

The applications of ferrofluids have been wide spread since their first appearance. Nowadays ferrofluids are being employed in aerospace systems such as propulsion and pumping, (Gontijo, 2013). In the medical field they can be used as drug carriers for high impact medications reducing collateral damage caused by them. Recent studies have shown that ferrofluids can also be used for hperthermia of tumours for cancer treatment (Seridonio and Fachini, 2010). Mechanical systems such as heat exchangers and dampers may be enhanced by employing this material as a medium. On heat exchangers thermomagnetic convection can be exploited enhancing heat transfer or even simulating gravity on weightless environments (Rlums, 1995). Active damping may be accomplished by pumping and controlling the fluid viscosity according to the system specification(Scherer and Neto, 2005).

2. Problem Formulation

The present work consists on a numerical study of the flow of a ferrofluid past a flat plate. The investigation of the magnetic effects on the boundary layer is done numerically using the vorticity - stream function method. For this purpose we consider that a fluid with density ρ and viscosity μ with an uniform velocity profile $u = U_\infty$ reaches a flat plate of length L. Here the two dimensional velocity field $\boldsymbol{u}$ is denoted by its components as $\boldsymbol{u} = u(x, y)\hat{e}_x + v(x, y)\hat{e}_y$. This fluid, with magnetic susceptibility χ is also subjected to an applied field $\boldsymbol{H}$ from a permanent magnet for example. Figure (1) shows a sketch of our problem.

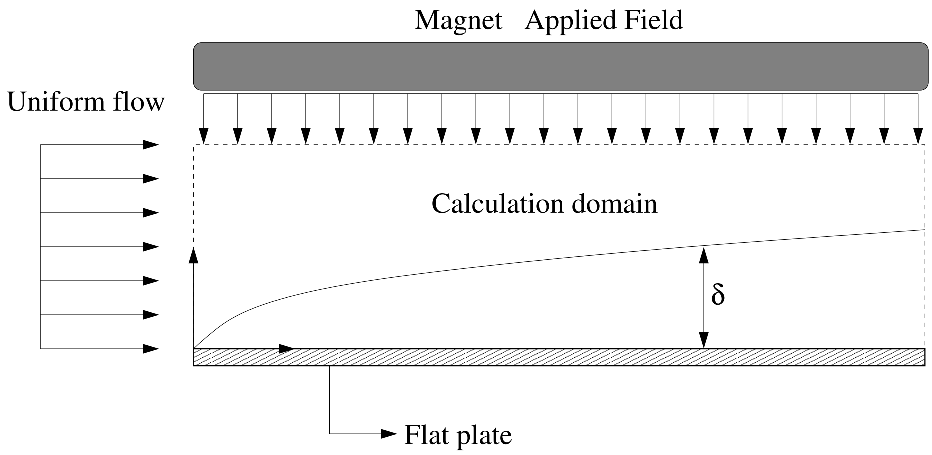

Figure 1. This picture shows a sketch of the studied problem. An uniform laminar flow of a magnetic fluid reaches a flat plate. At the same time we apply a magnetic field through a permanent magnetic on the upper boundary of the calculation domain. The velocity field is strongly influenced by magnetic effects.

2.1 Governing Equations

The physical model of ferrohydrodynamics consists on the coupling of the governing equations of hydrodynamics and the Maxwell's equations of electromagnetism. Since this field has not been established yet, there are still some open questions regarding the set of governing equations that rules the motion of ferrofluids under the presence of an applied field. The present work will be based on two different models for the magnetization, first a linear model (Rosenweig, 2014) and second a evolutive model (Shiliomis, 2001).

We start by stating the Maxwell's equations that will take part in the mechanics of a ferrofluid flow. Since most ferrofluid carriers are considered dieletric we may argue that no net current will be present in the flow, i.e $\mathbf{J} = 0$, being $\mathbf{J}$ the electric current density. This assumption is known as the *magnetostatic limit*. Ampére's circuit law in the magnetostatic limit takes the form

$$\nabla \times \boldsymbol{H} = 0, \tag{1}$$

where $\boldsymbol{H}$ represents the applied magnetic field. Equation (1) implies that the vector field $\boldsymbol{H}$ is irrotational therefore it can be expressed as the gradient of a scalar potential function, $\boldsymbol{H} = -\nabla\phi_m$, where

$$\nabla \times \nabla\phi_m = 0, \tag{2}$$

here ϕ_m is referred to as the magnetic potential field. The Gauss's law of magnetic induction states that no magnetic monopoles exist in our physical world and so the net flux of magnetic field over a closed surface must equals to zero, the differential form of this law is written as follows,

$$\nabla \cdot \boldsymbol{B} = 0. \tag{3}$$

In equation (3), $\boldsymbol{B}$ represents the induction field which is given by the vector sum of the the applied magnetic field $\boldsymbol{H}$ and the medium's capacity to polarize itself under the presence of a field $\boldsymbol{M}$, which is the flow magnetization, so

$$\boldsymbol{B} = \mu_0(\boldsymbol{H} + \boldsymbol{M}) \tag{4}$$

where $\mu_0 = 4\pi \times 10^{-7} N/A^2$ is the magnetic permeability of free space. Substituting equation 2 on 3 yields that,

$$\nabla^2 \phi_m = \nabla \cdot \boldsymbol{M}. \tag{5}$$

From equation (5) it is possible to determine the magnetic potential field throughout the whole domain of calculation. With the magnetic potential in hands the applied field is found by simply taking the gradient of it ($\mathbf{H} = -\nabla \phi_m$). For a superparamagnetic fluid with constant suceptibility the magnetic potential field is governed by Laplace's equation. A difficult numerical task is to propose consistent boundary conditions in terms of ϕ_m that would provide a physically consistent field $\boldsymbol{H}$. These conditions are usually expressed in terms of a Neumann boundary condition for ϕ_m (continuity of tangential components of $\mathbf{H}$) and must produce an irrotational applied field that satisfies the Ampère law in the magnetostatic regime. In the present work we want to focus our attention in the flow response to the presence of a given applied field. Our focus is to understand the route of possible instabilities in the flow field created by the imposition of an external applied magnetic field. The influence of the strength of the applied field on the velocity flow field will be investigated.

The applied field considered in the calculations of the present work is given by a rectangular permanent magnet placed underneath the the flow domain. The solution for this field for a superparamagnetic fluid with constant suceptibility is known (Clegg, 1987) and assumes the following dimensionless form

$$H_x = \frac{J}{4\pi\mu_0} \ln \left[\frac{y + b + \{(y+b)^2(x-a)^2\}^{\frac{1}{2}}}{y - b + \{(y-b)^2(x-a)^2\}^{\frac{1}{2}}} \times \frac{y - b + \{(y-b)^2(x+a)^2\}^{\frac{1}{2}}}{y + b + \{(y+b)^2(x+a)^2\}^{\frac{1}{2}}} \right] \tag{6}$$

and

$$H_y = \frac{J}{4\pi\mu_0} \ln \left[\frac{y + a + \{(y-b)^2(x+a)^2\}^{\frac{1}{2}}}{y - a + \{(y-b)^2(x-a)^2\}^{\frac{1}{2}}} \times \frac{y - a + \{(y+b)^2(x-a)^2\}^{\frac{1}{2}}}{y + a + \{(y+b)^2(x+a)^2\}^{\frac{1}{2}}} \right] \tag{7}$$

where H_x and H_y are the components of the field in directions x and y respectively, J is the polarization (μ_0 M) of the magnet) and x and y represent the coordinate of an arbitrary point within the calculation domain. Figure 2 shows a typical field line pattern for the applied magnetic field $\boldsymbol{H}$ in our calculation domain. Once again is important to emphasize that our goal is to avail the influence of a given field on the behavior of the hydrodynamic field when the fluid is sensible to magnetic effects. In other words, we will assume a simple field $\boldsymbol{H}$ and study the influence of hydrodynamic effects on the magnetization of the magnetic fluid and how it affects the velocity field. This work is a first approach of a more complicated problem, which should include the influence of the magnetization field on the magnetic potencial ϕ_m, through equation (5).

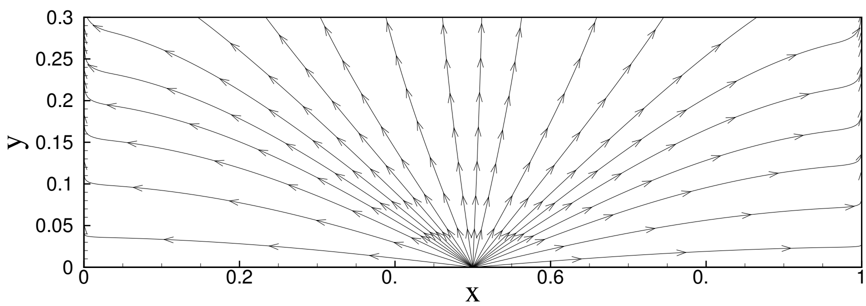

Figure 2. Stream line pattern for the applied magnetic field $\boldsymbol{H}$

In order to close our model we need make use of a magnetization model so that the we are able to link the physical quantities of our problem. First we present a linear magnetization model known as the superparamagnetic model proposes that the magnetization vector $\boldsymbol{M}$ has the following form,

$$\boldsymbol{M} = \chi \boldsymbol{H} \tag{8}$$

where χ is the magnetic susceptibility of the fluid. For a superparamagnetic fluid the particles magnetic memory is null so they respond instantly to the application of an external field $\boldsymbol{H}$. Under this condition the fluid magnetization vector $\boldsymbol{M}$ is considered to be always aligned to the applied field $\boldsymbol{H}$ so that $\boldsymbol{M} \parallel \boldsymbol{H}$. Second, we show a recent model for the magnetization (Shiliomis, 2001) that is given by,

$$\frac{\partial \boldsymbol{M}}{\partial t} + \boldsymbol{u} \cdot \nabla \boldsymbol{M} = \boldsymbol{\Omega} \times \boldsymbol{M} - \frac{1}{\tau} (\boldsymbol{M} - \boldsymbol{M}_0). \tag{9}$$

Equation 9 takes into account both internal magnetic and mechanical torques. The parameter τ represents the magnetic relaxation time and M_0 is the equilibrium magnetization of the media and is given by,

$$\frac{\boldsymbol{M}_0}{M_d\phi} = \mathcal{L}(\alpha)\hat{e}_H \tag{10}$$

where ϕ is the volume fraction of magnetic particles and M_d is the magnetization of the solid particles immersed on the fluid. The vector $\hat{e}_H$ is given by $\hat{e}_H = \frac{\boldsymbol{H}}{|\boldsymbol{H}|}$ and represents the direction of the magnetization vector. The term $\boldsymbol{\Omega}$ is given by

$$\boldsymbol{\Omega} = \frac{1}{2}\nabla \times \boldsymbol{u} + \frac{1}{\zeta}\boldsymbol{M} \times \boldsymbol{H}, \tag{11}$$

where ζ represents a typical magnetic relaxation time scale associated with a deviation from the condition of a symmetrical fluid. Here the word *symmetrical* is used in the sense of the stress tensor symmetry. We know that from the balance of angular momentum that $\boldsymbol{\varepsilon}\colon\boldsymbol{\sigma} = \boldsymbol{t}$. Here $\boldsymbol{\varepsilon}$ is the third order isotropic anti symmetric tensor (given in terms of Levi-Civita's permutation symbol ε_{ijk}. It is also instructive to define $\boldsymbol{t}$ as an internal torque density. This variable is only present in polar fluids. For a Newtonian fluid the balance of angular momentum states simply that $\boldsymbol{\varepsilon}\colon\boldsymbol{\sigma}$, so $\boldsymbol{\sigma} = \boldsymbol{\sigma}^T$. For a magnetic fluid the product $\boldsymbol{\varepsilon}\colon\boldsymbol{\sigma} \neq 0$, so $\boldsymbol{\sigma} \neq \boldsymbol{\sigma}^T$, thus we have that $\boldsymbol{\varepsilon}\colon\boldsymbol{\sigma} = -\mu_0\boldsymbol{M} \times \boldsymbol{H}$ which is the negative of the torque acting on the dipolar matter due to the presence of an applied field.(Rosenweig, 2014)

Since ferrofluids are liquid colloids, we may say that in general they will behave as an incompressible media, so in other words we can say that their density is constant. We introduce here the continuity equation of incompressible fluids,

$$\nabla \cdot \boldsymbol{u} = 0, \tag{12}$$

where $\boldsymbol{u}$ is the Eulerian velocity field of the flow. The equation that governs the mechanics of fluid motion (balance of linear momentum) can be written in a general form as follows,

$$\rho\left(\frac{\partial \boldsymbol{u}}{\partial t} + \boldsymbol{u}\cdot\nabla\boldsymbol{u}\right) = \nabla\cdot\boldsymbol{\sigma} + \mathbf{f}, \tag{13}$$

where t represents time, $\boldsymbol{\sigma}$ are the stresses acting on an infinitesimal continuum fluid volume and $\mathbf{f}$ represents body forces. Equation 13 represents the balance of linear momentum in a continuum infinitesimal volume. The L.H.S of the equation represents the local variation and the advective transport of linear momentum in the flow. On the R.H.S we have the divergent of the stress tensor that represents the surface forces and $\mathbf{f}$ representing the action of body forces. In ferrohydrodynamics the effects of gravitational forces are not of significant relevance so the term $\mathbf{f}$ may be neglected. Now we turn our attention to the stress tensor $\boldsymbol{\sigma}$, that can be decomposed into two parts,

$$\boldsymbol{\sigma} = \boldsymbol{\sigma}^H + \boldsymbol{\sigma}^M \tag{14}$$

where $\boldsymbol{\sigma}^H$ represents the hydrodynamical surface forces given by

$$\boldsymbol{\sigma}^H = -p\mathbf{I} + 2\eta\mathbf{D} \tag{15}$$

The magnetic effects are taken into account by $\boldsymbol{\sigma}^M$, and is written as

$$\boldsymbol{\sigma}^M = -p_m\mathbf{I} + \boldsymbol{HB} \tag{16}$$

where $-p_m$ represents the magnetic pressure given by $\frac{1}{2}\mu_0|\boldsymbol{H}|^2$. Similarly the term $\boldsymbol{HB}$ accounts for the magnetic stresses on the fluid volume. The term $\boldsymbol{HB}$ is related to tangential and normal surface forces acting on a fluid particle due to the presence of an applied field. This field is able to change the suspension's micro structure and by consequence producing anisotropic stresses inside the material. The final form of the momentum transport equation is given by,

$$\rho\left(\frac{\partial \boldsymbol{u}}{\partial t} + \boldsymbol{u}\cdot\nabla\boldsymbol{u}\right) = -\nabla p + \eta\nabla^2\boldsymbol{u} + \mu_0\boldsymbol{M}\cdot\nabla\boldsymbol{H} + \nabla\times(\boldsymbol{M}\times\boldsymbol{H}). \tag{17}$$

Since the flow is incompressible i.e $\nabla\cdot\boldsymbol{u} = 0$, we may introduce a stream function ψ that satifies the relation for a 2D field,

$$\boldsymbol{u} = \nabla\times\psi\hat{e}_z. \tag{18}$$

By definition the vorticity of the flow $\boldsymbol{\xi}$ is given by

$$\boldsymbol{\xi} = \nabla\times\boldsymbol{u} \tag{19}$$

substituting equation 18 into equation 19 and using the vector identity $\nabla \times \nabla \times \mathbf{A} = \nabla(\nabla \cdot \mathbf{A}) - \nabla^2 \mathbf{A}$ we get the poison equation for the stream function,

$$\nabla^2 \psi = -\xi_z. \tag{20}$$

By taking the curl of the momentum transport equation we have,

$$\rho \left(\frac{\partial \boldsymbol{\xi}}{\partial t} + \boldsymbol{u} \cdot \nabla \boldsymbol{\xi} \right) = \eta \nabla^2 \boldsymbol{\xi} + \mu_0 \left[\nabla \times (\boldsymbol{M} \cdot \nabla \boldsymbol{H}) - \nabla^2 (\boldsymbol{M} \times \boldsymbol{H}) \right]. \tag{21}$$

When imposing the super paramagnetic hypothesis 5 in order to simplify equation 21 a limitation of the vorcity-stream function comes up since our vorticity equation reduces to a simple Newtonian fluid case

$$\rho \left(\frac{\partial \boldsymbol{\xi}}{\partial t} + \boldsymbol{u} \cdot \nabla \boldsymbol{\xi} \right) = \eta \nabla^2 \boldsymbol{\xi}. \tag{22}$$

This is physically congruent with the phenomena described by the conservation of angular momentum for a magnetic fluid (16) which states that $\boldsymbol{\varepsilon} \colon \boldsymbol{\sigma} = \mu_0 \mathbf{M} \times \mathbf{H}$. When the super paramagnetic hypothesis is assumed ($\mathbf{M} = \chi \mathbf{H}$) the magnetic tensor stress tensor becomes symmetric and is not capable of producing internal toques thus the vorticity dynamics is not altered by the presence of the magnetic field.

2.2 Dimensionless form of the governing equations

The governing equations can be reduced to a dimensionless form if the typical scales are provided. By setting a the typical scales U_∞ for velocity, l for length and H_0 for the magnetic field. The dimensionless governing equations for the vorticity and stream function are,

$$\frac{\partial \boldsymbol{\xi^*}}{\partial t^*} + \boldsymbol{u^*} \cdot \nabla^* \boldsymbol{\xi^*} = \frac{1}{Re} \nabla^{2*} \boldsymbol{\xi^*} + \frac{1}{Re_m} \left[\nabla^* \times (\boldsymbol{M^*} \cdot \nabla^* \boldsymbol{H^*}) - \nabla^{2*} (\boldsymbol{M^*} \times \boldsymbol{H^*}) \right]. \tag{23}$$

$$\nabla^{2*} \psi^* = -\xi_z^* \tag{24}$$

The variables with a (*) superscript are the new dimensionless variables. The term Re corresponds to the Reynolds number given by $Re = \frac{U_\infty L}{\nu}$. Similarly the magnetic Reynolds number is written as $Re_m = \frac{\rho U_\infty^2}{\mu_0 H_0^2}$. The magnetic Reynolds number expresses a relation between inertial and magnetic forces. The evolutive magnetization equation 12 is rewritten into,

$$\frac{\partial \boldsymbol{M}^*}{\partial t^*} + \boldsymbol{u}^* \cdot \nabla^* \boldsymbol{M}^* = \boldsymbol{\Omega}^* \times \boldsymbol{M}^* - \frac{1}{\tau^*} (\boldsymbol{M}^* - \boldsymbol{M}_0^*) \tag{25}$$

where $\Omega^* = \frac{1}{2} \nabla^* \times \boldsymbol{u}^* + \frac{1}{\zeta^*} \boldsymbol{M}^* \times \boldsymbol{H}^*$ represents the dimensionless precession term.

3. Numerical Model

The solution method employed in this work was the vorticity-stream function method. The governing equations are discretized using finite differences (Smith, 1978) grid where all the variables are evaluated at the same nodes. The transient terms are discretized in a up wind difference scheme (UDS),for the advective terms back wind difference scheme (BDS) is used while the diffusive terms are discretized in a central difference scheme (CDS). The solution of the velocity field is found indirectly at each time step by solving equation 19. In the case of super paramagnetic magnetization the algorithm consists on solving the following equations until convergence is reached.

$$a_p \boldsymbol{\xi}_p^{t+1} = \Sigma a_n \boldsymbol{\xi}_n^t + s_n^t \tag{26}$$

$$b_p \psi_p^{t+1} + \Sigma b_n \psi^{t+1} = \psi_p^{t+1} \tag{27}$$

For the evolutive magnetization problem, equation 9 is discretized in the same fashion as equation 21. The discretized magnetization equation equation is added to to the algorithm in the following form,

$$c_p \boldsymbol{M}_p^{t+1} = \Sigma c_n \boldsymbol{M}_n^t + r_p^t \tag{28}$$

where

$$\boldsymbol{M} = \left[\begin{array}{c} M_x \\ M_y \end{array} \right] \tag{29}$$

where equation 28 is solved at each time stem along equations 26 and 27.

The convergence criteria for the solutions was defined after successive trials of different values of tolerance ϵ, ranging from 10^{-2} to 10^{-9}. Choosing any value bellow 10^{-6} has shown no significant improvement on the solution so we defined $max(|u^{t+1} - u^t| < 10^{-6})$ as our final convergence test. When this value is smaller than a tolerance ε we consider that the simulation has reached a steady state regime and thus it stops.

In order to provide a simple mesh study we show figure 3. This figure shows the relative error $\epsilon = \frac{\delta_n - \delta_e}{\delta_e}$ of both boundary layer thickness and drag coefficient at the plate mid point ($x = 0.5$) as a function of the number of nodes used on the calculation grid. Here the lower index e represents the exact solution (Blasius, 1908) and the lower index n denotes the numerical solution. The grid configurations tested in this analysis were $[20\times 50, 30\times 50, 30\times 60, 30\times 70, 30\times 80, 40\times 80]$ and they refer to numbers $[1, 2, 3, 4, 5, 6]$ in figure 3.Since the error values seemed to be stable at 6, a grid 40×80 was used for all calculations in this paper. It is also important to say that it was decide to use a greater number of nodes in direction y (perpendicular to the flow field). In this sense the mesh is finer in the direction where the derivatives associated with the influence of the wall are higher.

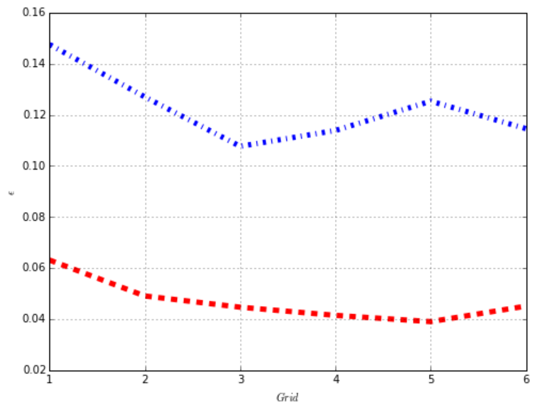

Figure 3. The blue lines represent the relative error in the boundary layer thickness δ while red lines show the the relative error in the drag coefficient C_f for a given grid set up.

4. Results

We start presenting figures (4) and (5). These figures illustrate the velocity field behaviour for both, a super paramagnetic fluid and an asymmetric magnetic fluid, under the presence of an applied field. The field is generated by a permanent magnet placed immediately underneath the plate. The magnetic field lines for the applied magnetic field were already shown in figure (2). In both figures (4) and (5) the behaviour of the velocity field is taken under the same Reynolds number $Re = 1000.0$, and magnetic Reynolds $Re_m = 5.0$. For the supeparamagnetic model a magnetic susceptibility of $\chi = 0.5$ is used, for the aymmetric model model the parameters were chosen as $\alpha = 1.0$, $\tau = 1.0$, $\zeta = 1000.0$, $M_d = 1.0$ and $\phi = 0.01$.

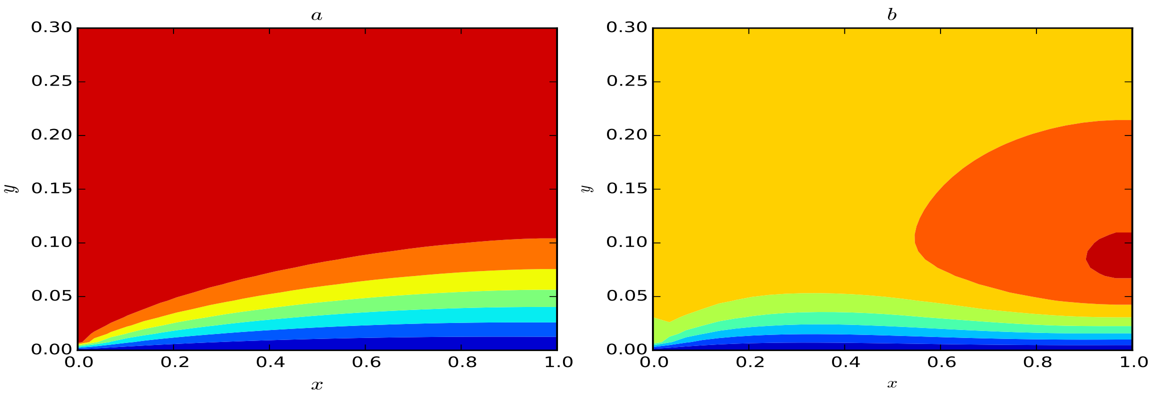

Figure 4. Velocity field in the x direction for $Re_m = 5.0$ in different magnetization regimes. (a) superparamagnetic, (b) asymmetric magnetic fluid.

From figures (4) and (5) we may infer that the application of an external field may be used in order to control the boundary layer thickness and the drag force, but also to provide new nonlinear instabilities in the flow field. These instabilities could be used for example to increase the heat transfer rates in practical problems. A very interesting work on the theme was made recently by (Gontijo and Cunha, 2012), in this work the authors have used a low volume fraction magnetorheological suspension and were able to increase in up to 20% the heat transfer rates inside a thin retangular cavity with an applied permanent neodimium magnetic. One can also notice that the difference on the qualitative behaviour of both models is more prominent at the end of the plate. Since viscous effects are acumulated as the fluid passes through the plate, we may infer that the role of vorticity at the end of the calculation domain (near the wall) is responsible for the deviation between the fields shown in figures (4a) and (5a) from the ones at figures (4b) and (5b).

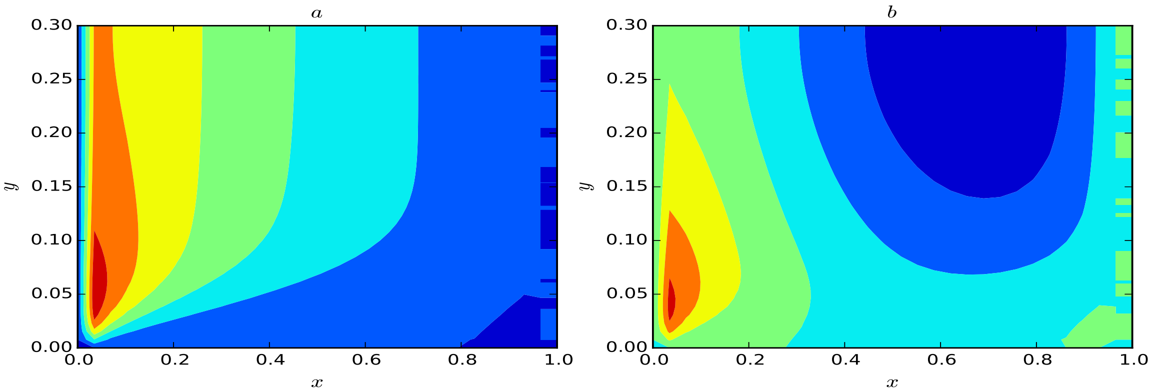

Figure 5. Velocity field in the y direction for $Re_m = 5.0$ in different magnetization regimes. (a) superparamagnetic, (b) asymmetric magnetic fluid.

Figures (6) and (7) show the steady state magnetization field in both x and y directions for both models.

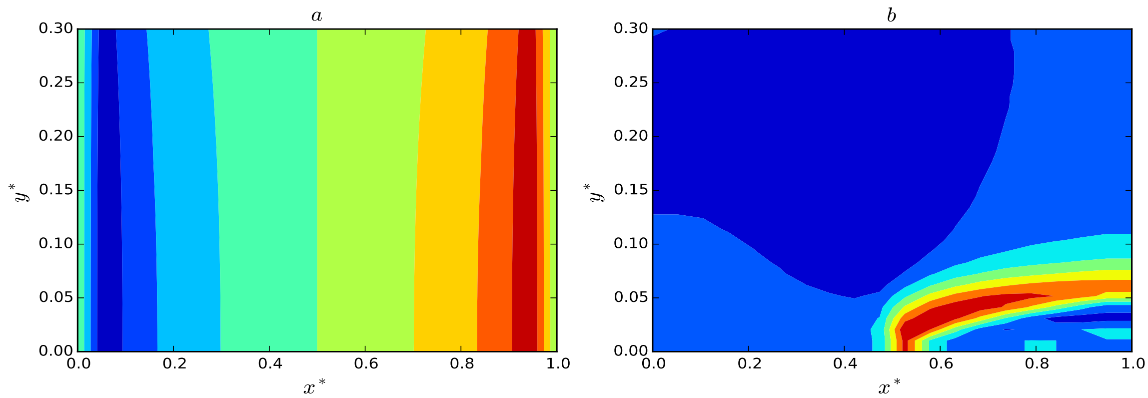

Figure 6. Magnetization field in the x direction for $Re_m = 5.0$ in different magnetization regimes. (a) superparamagnetic, (b) asymmetric magnetic fluid.

While symmetry is conserved in figures (6a) and (7a) for a super paramagnetic fluid, the asymmetric fluid shown in figures (6b) and (7a) is clearly under the influence of magnetic torques (absent in the superparamagnetic model) and also hydrodynamic effects of vorticity and convection that cause the refered symmetry breaking in the magnetization pattern. This behavior is even clear in figures (8) and (9).

Indeed, when we consider a superparamagnetic fluid, the magnetization field is not coupled with the flow velocity field. Instead it is simply aligned with the applied field, as if the fluid were a static medium. Physically this only happens when the magnetic time scale is much smaller than any hydrodynamic time scale and so the particles are always aligned with the applied field. Several transport mechanisms are not considered within the superparamagnetic approach. Among these mechanisms we may highlight the advective transport, a linear magnetic relaxation due to the term $1/\tau^* \, (\boldsymbol{M}^* - \boldsymbol{M}_0^*)$, the influence of magnetic torques $1/\zeta^* \, (\boldsymbol{M}^* \times \boldsymbol{H}^*) \times \boldsymbol{M}^*$ and the fluid vorticity $1/2(\nabla \times \boldsymbol{u}^*) \times \boldsymbol{M}^*$. Since the magnetic is applied underneath the plate the influence of magnetic torques and the flow vorticity is more intense near the wall. However the advective contribution is more prominent in the beginning of the plate and hence it ends up moving the low magnetization field area to the near wall region at the end of the calculation domain. This lower magnetization area is located in the region $0.5 \leq x \leq 1$ for $0 \leq y \leq 0.05$.

It is interesting to notice that $\boldsymbol{M} \parallel \boldsymbol{H}$ for a superparamagnetic fluid. Since the external field is irrotational, the magnetic potential ϕ_m is ruled by Laplace's equation ($\nabla^2 \phi_m = 0$) for the free space. The elliptic nature of a field

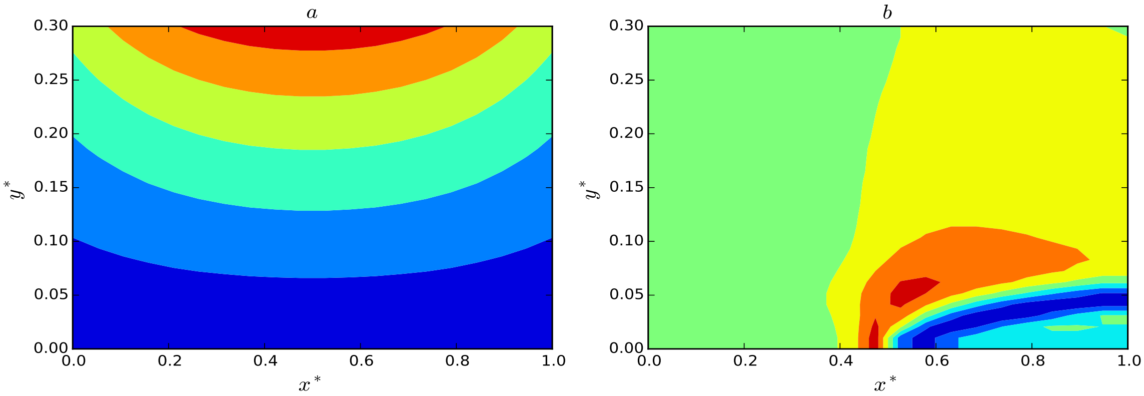

Figure 7. Magnetization field in the y direction for $Re_m = 5.0$ in different magnetization regimes. (a) superparamagnetic, (b) asymmetric magnetic fluid.

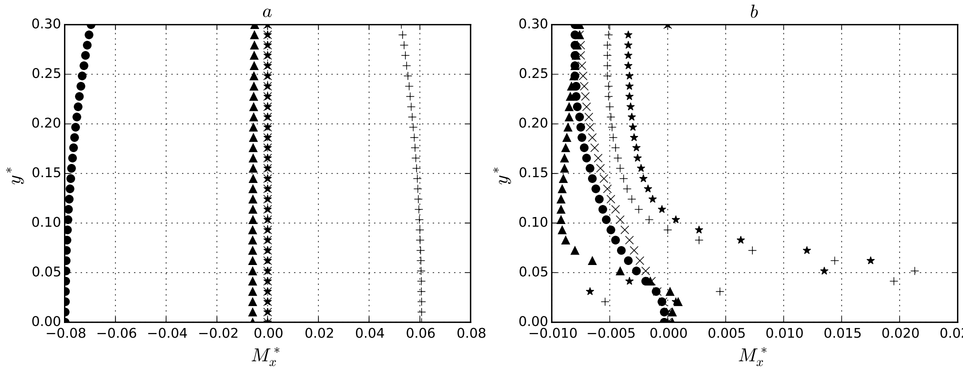

Figure 8. Shows the magnetization at the x direction M_x^* for (a) Super Paramagnetic Model and (b) Evolutive Magnetization Model. Each symbol represents a different a different position on the horizontal direction (x), $x = 0.0$ for $\times$, $x = 0.25$ for $\circ$, $x = 0.5$ for $\triangle$, $x = 0.75$ for $+$ and $x = 1.0$ for $*$

described by Laplace's equation is clearly seen in picture (7a), while the parabolic nature of the advective transport is highly prominent in figure (7b).

In order to see how the applied field affects the overall behaviour of the hydrodynamic field , we plot figure (10). This plot shows the behaviour of the boundary layer thickness and drag coefficient over the plate for both models of magnetization for a constant magnetic Reynolds number $Re_m = 5.0$. In figure (10a) the boundary layer thickness is shown and compared to the analytical result and in figure (10b) we show how the local drag coefficient varies along the plate for both magnetization models. We observe an increased drag followed by a shrinking of the boundary layer due to magnetic effects on both cases. The effect of magnetic forces acting on the fluid appears to be slowing down the flow near the flat plate causing a greater velocity gradient normal to the wall and a thinner boundary layer. This behaviour is consistent with the intuitive thought that if we place a permanent magnet under a flat plate it would tend to drag the fluid to its direction. The aggregative nature of magnetic interaction has been extensively explored by (Gontijo and Cunha, 2015) and this nature is responsible for the decrease in the boundary layer thickness and the consequent increase in the drag coefficient when the field is applied.

An interesting observation is the fact that the solution of a magnetization evolutive equation involves other parameters when compared to the supeparamagnetic regime. For instance the only input used to calculate the magnetization field for the supeparamagnetic case is the magnetic suceptibility χ. For the asymmetric case (magnetization evolutive equation) we have ϕ, α, τ^*, ζ^* and M_d^*. In this sense we can not guarantee that the comparison shown in pictures (10) and (11) is done under the same physical values of the time scales involved in the problem. However, the qualitative behavior shown in both cases is the same. The application of a magnetic field in the lower boundary of the calculation domain is responsible for a decrease on the boundary layer thickness, which is followed by an increase in the drag coefficient.

5. Conclusion

In this work we presented a first glimpse on how a magnetic field interacts with the flow of a ferromagnetic fluid and vice versa. The focus of this work was to compare the effects of a superparamagnetic model in the flow field of a

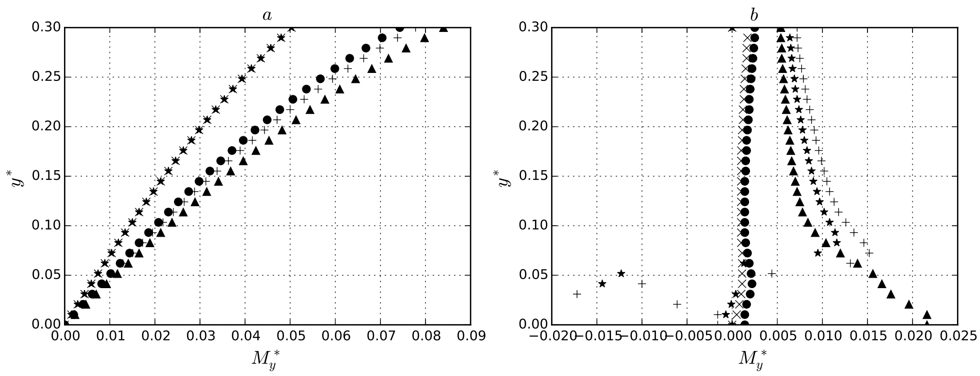

Figure 9. Shows the magnetization at the y direction M_y^* for (a) Super Paramagnetic Model and (b) Evolutive Magnetization Model. Each symbol represents a different a different position on the horizontal direction (x), $x = 0.0$ for $\times$, $x = 0.25$ for $\circ$, $x = 0.5$ for $\triangle$, $x = 0.75$ for $+$ and $x = 1.0$ for $*$

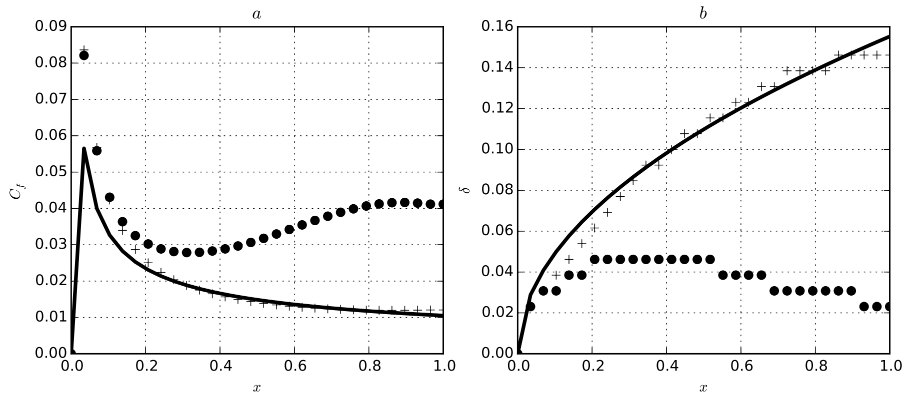

Figure 10. Shows (a) the drag coefficient C_f and (b) the boundary layer thickness δ . Each symbol represents a different a different magnetization model where (a) $+$ is used for the Super Paramagnetic Model and (b) $\circ$ is used for the Evolutive Magnetization Model.

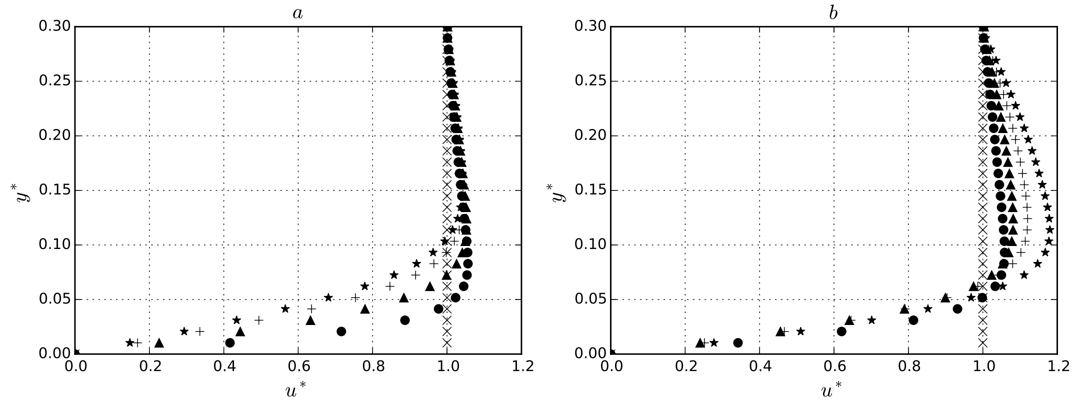

Figure 11. Shows the streamwise velocity u^* for (a) Super Paramagnetic Model and (b) Evolutive Magnetization Model. Each symbol represents a different a different position on the horizontal direction (x), $x = 0.0$ for $\times$, $x = 0.25$ for $\circ$, $x = 0.5$ for $\triangle$, $x = 0.75$ for $+$ and $x = 1.0$ for $*$

magnetic fluid flow over a flat plate. In this sense we focused our attentions in understanding how the coupling of vorticity with magnetization and other transport mechanisms such as advection and internal magnetic torques may alter the flow field. Since most of the current research works on the field of ferrohydrodynamics consider the superparamagnetism simplification, we tryied to investigate what physical mechanisms this assumption may hide.

We have seen that the solution of an evolutive equation for the magnetization field provides a meaningful deviation of the supeparamagnetic regime. Not only in terms of symmetry breaking but also in terms of the overall structure of the laminar boundary layer development for a magnetic fluid. For instance we have seen that the lower magnetization area near the wall at the end of the plate is responsible for a significant decrease on the boundary layer thickness when compared to the superparamagnetic case.

Although the asymmetric magnetization model has shown some interesting coupling mechanisms with the flow field, considering both mechanisms of vorticity and advection, the drag increase due to magnetic interactions may be subject to further investigations. In this sense this mechanism may be exploited in drag control systems in the future. Also further studies may be done on the heat transfer properties using a heated plate.

6. References

Acheson, D.J., 2009. "Elementary fluid dynamics". *Oxford University Press*.

Blasius, H., 1908. "Grenzschichten in flussigkeiten mit kleiner reibung". *Z. Math. Phys. 56: 1-37*.

Clegg, A.G., 1987. "Permanent magnets in theory and practice". *Pentech Press*.

Gontijo, R.G., 2013. "Micromecânica e microhidrodinâmica de suspensões magnéticas". *Tese de Doutorado, Universidade de Brasília*.

Gontijo, R.G. and Cunha, F.R., 2012. "Experimental investigation on thermo-magnetic convection inside cavities". *Journal of Nano Science and Nanotechnology, Vol. 12, 9198-9207*.

Gontijo, R.G. and Cunha, F.R., 2015. "Dynamic numerical simulations of magnetically interacting suspensions in creeping flow". *Powder Technology, Vol 279 (DOI: 10.1016/j.powtec.2015.03.033), 146-165*.

Granger, R.A., 1997. "Fluid mechanics". *Dover Publications*.

Rlums, E., 1995. "New applications of heat and mass transfer processes in temperature sensitive magnetic fluids". *Brazilian Journal of Physics, Vol. 25, 2: 112-117*.

Rosenweig, R.E., 2014. "Ferrohydrodynamics". *Dover Publications*.

Scherer, C. and Neto, A.M.F., 2005. "Ferrofluids: Properties and applications". *Brazilian Journal of Physics, Vol. 35, no. 3A*.

Schlichting, H., 2000. "Boundary layer theory". *Springer*.

Seridonio, A.C. and Fachini, F.F., 2010. "Heat dissipation in liquid with magnetic nanoparticles in the presence of a circular polarized field and vorticity". In *VI NATIONAL CONGRESS OF MECHANICAL ENGINEERING, 1-6*.

Shiliomis, M., 2001. "Ferrohydrodynamics: Testing a third magnetization equation". *Physical Review E, Vol. 64, p.060501(R)*.

Smith, G.D., 1978. "Numerical solution of partial differential equations: Finite difference methods". *Oxford University Press*.

Stephen, P., 1965. "Low viscosity magnetic fluid obtained by the colloidal suspension of magnetic particles". URL `https://www.google.com/patents/US3215572`. US Patent 3,215,572.

7. RESPONSIBILITY NOTICE